Effect of Molecular Weight of Polyethylene Glycol on Copper Electrodeposition in the Presence of Bis-3-Sulfopropyl-Disulfide

Sol-Ji Song[1], Seok-Ryul Choi[1], Jung-Gu Kim[1,], Ho-Gun Kim[2]*

[1] School of Advanced Materials Science and Engineering, Sungkyunkwan University, 300 Chunchun-Dong, Jangan-Gu, Suwon 440-746, Republic of Korea
[2] LG R&D Copmlex, 555, Hogye-Dong, Dongan-Gu, Anyang 431-080, Republic of Korea
*E-mail: kimjg@skku.edu

This study examined the effect of polyethylene glycol (PEG) with different molecular weights on the copper electrodeposition in acid copper sulfate plating solution containing bis-3-sulfopropyl-disulfide (SPS) and chloride ion. Quantum chemical study, cyclic voltammetry, and surface analyses (HP-thin film XRD, FE-SEM) were conducted to evaluate the adsorption nature, crystallographic characteristics, and surface morphology. In copper electrodeposition, the adsorption effect of PEG is dependent on its molecular weight regardless of the existence of SPS. The increase of suppression effect with high PEG molecular weight induced the SPS biasing action which causes the change of surface property such as roughness, glossiness, preferred plane and grain size. In addition, PEG activated SPS reactions.

1. INTRODUCTION

Electrodeposition is an electrochemical process of metal coating onto a conductive substrate immersed in electrolyte solution by applying a current [1,2]. Among various electrodeposition materials, copper is utilized due to its high thermal and electrical conductivity. Copper has been traditionally used in electronic products such as printed circuit boards (PCBs) and semiconductor devices [3-5]. Recently, with the development in the electronic industry, ultra-high frequency (about 10 GHz) is required for the transmission line. To get the ultra-high frequency, it is essential to reduce surface resistance and signal attenuation which are affected by surface roughness [6-9].

Copper sulfate plating solution is composed of inorganic and organic additives that can affect the surface roughness, morphology, and crystallographic property [1,5,10]. Its inorganic components include copper sulfate, sulfuric acid, and halogen ions. Chloride ion (Cl^-) is an indispensable component of copper sulfate plating solution. It acts as an electron bridge for copper ion reduction and leads to interactions with organic additives in the solution [11-14]. The organic additives can be classified as accelerator, suppressor, and leveler based on their influence on copper electrodeposition kinetics.

Bis-3-sulfopropyl-disulfide (SPS) is one of the typically used organic additives. Tan et al. [15] have reported that SPS can inhibit copper deposition in the absence of Cl^-. In the presence of Cl^-, the participation in the charge transfer process makes SPS an accelerator by increasing the rate of copper reduction.

Polyethylene glycol (PEG) is a typical suppressor that can inhibit copper reduction rate. PEG has a wide range of molecular weight (MW). Therefore, several studies have been conducted on its MW and characteristics of electrodeposition. Ko et al. [16] have studied suitable MW and concentration of PEG by electrochemical measurement. Manu et al. [17] have shown that the MW of PEG can affect the crystallographic orientations of deposited copper. Specifically, with increase in MW of PEG, the major plane measured by XRD is changed from 220 to 111. High MW PEG has a large adsorption capacity especially at plane 111 due to its low surface energy compared to other planes. Because adsorbed PEG can induce the cathode over-potential, the major plane is changed to 111. However, the effect of PEG MW when PEG co-exists with other organic additives in the solution has not been determined yet. Organic additives are generally used in combination because acceleration reaction can induce bumpy surface while suppression reaction will retard the deposition of the copper [18]. PEG as a suppressor is used with SPS as an accelerator in industrial situation to control copper plating surface and rate. It is important to identify the inhibition effect of PEG MW when it co-exists with SPS to reflect industrial situation. Therefore, the objective of this study was to evaluate the effect of MW of PEG with SPS on deposited copper surface properties. For this objective, quantum chemical study and electrochemical cyclic voltammetry (CV) were conducted to evaluate adsorption nature of SPS and MW of PEG. Electrodeposition was performed in galvanostatic mode to apply current step-by-step. After electrodeposition, the surface property was analyzed. Changes in preferential plane and grain size of electrodeposited copper were confirmed using high power thin film X-ray diffraction (HP-thin film XRD). The surface morphology was observed through field emission scanning electron microscopy (FE-SEM).

2. EXPERIMENTAL

The electronic properties of SPS and PEG with different MWs were evaluated to analyze the adsorption property of the copper surface. Calculations were performed using B3LYP with base set 6-31+G(d,p) [19]. Quantum chemical calculations were carried out using GAUSSIAN-09 program. Molecular graphics were produced using Gauss-View 5.0 graphical package.

Cyclic voltammetry (CV) was measured to confirm the adsorption ability of different MW PEG with SPS using multi-potentiostat / galvanostat VSP-300. In CV test cell, a copper seed layer (0.49 cm^2), a saturated calomel electrode (SCE), and a platinum wire (1.507 cm^2) were used as working, reference, and counter electrode, respectively as the three-electrode electrochemical system. The copper seed layer was produced using sputtering method with a thickness of 0.1~0.3 μm on polymer. The CV experiment was performed with potential range from -1.0 V_{SCE} to 0 V_{SCE} and scan rate of 50 mV/s. The compositions of plating electrolyte were copper sulfate ($CuSO_4·5H_2O$), sulfuric acid (H_2SO_4), and Cl^-. Organic additives, SPS as an accelerator, and PEG as a suppressor with different MWs (300, 1000, 3400) were added to the electrolyte in the same amount. CV measurement was carried out in 500 mL solution that was maintained at 39 °C.

Copper foil was electrodeposited onto copper seed layer using galvanostatic mode. The experimental system of copper electrodeposition was composed of cathode, anode, electrolyte, thermometer, and air bubbling system. The cathode was a copper seed layer. The anode was an iridium-coated titanium plate. The distance between cathode and anode was fixed to maintain a constant current density. The concentration and temperature conditions of 2000 mL electrolyte were exactly the same as those used in the CV system. The electrolyte was agitated with air bubbling system to reduce the diffusion layer thickness (δ) for increasing electrodeposition efficiency. In order to reflect the condition similar to the actual electrodeposition process, the current was applied to the cathode step-by-step until a thickness of about 8 μm electrodeposited copper was achieved. After the electrodeposition of copper foil, electrodeposited copper was washed twice with distilled water to remove the remaining copper plating solution and dried using a drying machine.

Electrodeposited copper is known to undergo self-annealing or recrystallization at room temperature and it makes the difference in microstructures and mechanical performance [20-23]. For this reason, all electrodeposited specimens were subjected to surface analysis after storing at room temperature for 48 hours. The surface roughness was examined using an illuminometer (Mitutoyo SJ-210) with the sensitivity of 0.5 μm. Ten-point average roughness (R_z) was recorded. The glossiness was examined using a glossmeter (C.T YG-SM). Average values of surface roughness and glossiness were obtained from 5 times of measurements. HP-thin film XRD (Bruker D8 ADVANCE) was performed to measure the changes in preferential plane and grain size. The scan rate of XRD was 3° per min from 30° to 100° with an 18 kW Cu Kα X-ray. Top views and tilted views of electrodeposited copper were characterized using FE-SEM (JEOR JSM7500F) and FE-SEM (JEOR JSM7000F), respectively.

3. RESULTS AND DISCUSSION

3.1. Quantum chemical analysis

To simplify the investigation regarding the inhibition effect of PEG with different MW on copper electrodeposition, simulation was performed as shown in Figure 1 and Table 1. The quantum chemical analyses based on hard and soft acid and bases (HASB) principle were focused on the

following electronic structure parameters: energy of the highest occupied molecular orbitals (E_{HOMO}), energy of the lowest occupied molecular orbitals (E_{LUMO}), and energy band gap ($\Delta E = E_{LUMO} - E_{HOMO}$). Results are summarized in Table 2.
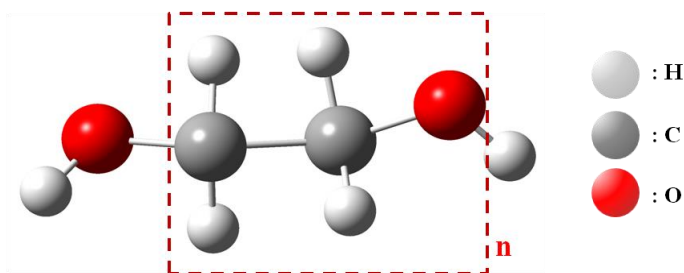

Figure 1. Simulated molecular structures of PEG.

Table 1. Simulated molecular weights of PEG

n	*Molecular weight*
2	106
4	194
10	458

Table 2. Quantum chemical parameters of PEG with different n: orbital energies of HOMO (E_{HOMO}), LUMO (E_{LUMO}), the LUMO-HOMO gap ($\Delta E = E_{LUMO} - E_{HOMO}$)

n	E_{HOMO} (eV)	E_{LUMO} (eV)	ΔE (eV)
2	-5.369	-3.009	2.360
4	-4.824	-3.596	1.228
10	-4.578	-3.649	0.929

Table 3. Quantum chemical parameters of SPS: orbital energies of HOMO (E_{HOMO}), LUMO (E_{LUMO}), the LUMO-HOMO gap ($\Delta E = E_{LUMO} - E_{HOMO}$)

	E_{HOMO} (eV)	E_{LUMO} (eV)	ΔE (eV)
SPS	0.664	1.631	0.967

E_{HOMO} is related to the electron-donating ability of the molecule. The higher the value of E_{HOMO}, the more molecules with tendency to donate electrons to appropriate acceptor molecules with low-energy empty molecular orbital. On the other hand, E_{LUMO} is related to the electron-accepting ability. As a result, the lower absolute value of the energy gap, the higher electron sharing properties between inhibitors and metal surface, thus better inhibitor efficiencies [24-27]. When the PEG MW was higher, the E_{HOMO} value was higher while the E_{LUMO} and ΔE values were lower. That is, the adsorption effect on copper layer is larger at higher MW of PEG.

When Cl⁻, SPS, and PEG co-exist, SPS and PEG are competitively adsorbed onto the copper seed layer. The SPS reacts as an accelerator after penetrating the PEG - Cu^+ - Cl⁻ complex [12,20]. Therefore, quantum chemical analysis was conducted for SPS. Results are shown in Table 3. The E_{HOMO} and E_{LUMO} values of SPS were higher compared to PEG, indicating that SPS has a strong tendency to donate electron but a weak tendency to accept electron. This is the reason why SPS is adsorbed with sulfonic end group that is negatively charged [28,29]. Based on quantum chemical results, the SPS would not be absorbed onto the copper surface. Instead, it reacted with cation such as the copper ion. Thus, SPS can accelerate the reduction reaction of copper ions. The ΔE value of SPS was lower except that when n was equal to 10, indicating that the degree of competitive adsorption between SPS and PEG is different according to the MW of PEG. Thus, the SPS adsorption is more difficult when the PEG MW is higher. However, because the adsorption mechanism of SPS is a chemical adsorption, it can be adsorbed onto copper [29].

3.2. Electrochemical measurements of PEG on copper surface

The effect of adsorption on different MWs of PEG with SPS is shown in Figure 2.
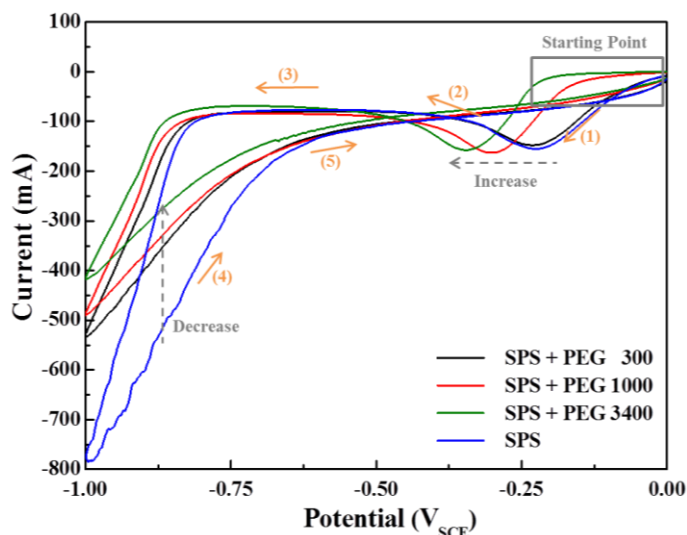

Figure 2. Result of CV with SPS and different MW of PEG in acid copper sulfate plating solution containing the chloride ion.

The result is shown in accordance with the number sequences. At the starting point of CV, the length of the region that appeared to have constant current with potential change was different. Large MW PEG showed longer region. It signifies the adsorption of PEG because the constant current means the disturbance to copper electrodeposition. However, the regions are hardly appeared with the addition of only SPS and PEG 300. As the MW of PEG was increased, the first peak at about -150 mA was shifted to a more negative potential because the suppression effect was larger for higher MW. These results were similar to those of quantum chemical analysis, although the CV solution contained not only PEG, but also SPS. Thus, the adsorption of PEG is unrelated to the presence of SPS. In the

absence of PEG, peak potential was similar to that of PEG 300 because the difference of ∆E between SPS and PEG 300 calculated by quantum chemical was very small. The suppression effect of PEG 300 was hardly observed at low potential area.

At high potential area (about -1.0 V_{SCE}), the absolute values of peak current were getting smaller as the MW of PEG was increased. Since the current represents movement of electrons, the magnitude of the current means the amount of copper ions deposited onto the copper seed layer. Low MW PEG had a small effect on the copper electrodeposition suppression. Therefore, the amount of deposited copper ions was increased at low MW PEG compared to that at high MW PEG. At backward scanning region from -1.0 V_{SCE} to 0 V_{SCE} (the region marked as (4) and (5)), CV showed a different suppression effect with PEG at a constant current. At the constant current, different MWs of PEG show different potentials. Higher MW of PEG shows lower potential. With the injection of additives sequentially under constant current conditions, the additives can be classified into potential changes [30,31]. If the injected additive has greater inhibition effect, it shows more drop in the potential. However, acceleration effect shows an increased potential. Because lower potential means greater inhibition at the constant current, the higher MW of PEG will increase the inhibition effect. Because SPS is an accelerator, it showed the highest potential at the constant current.

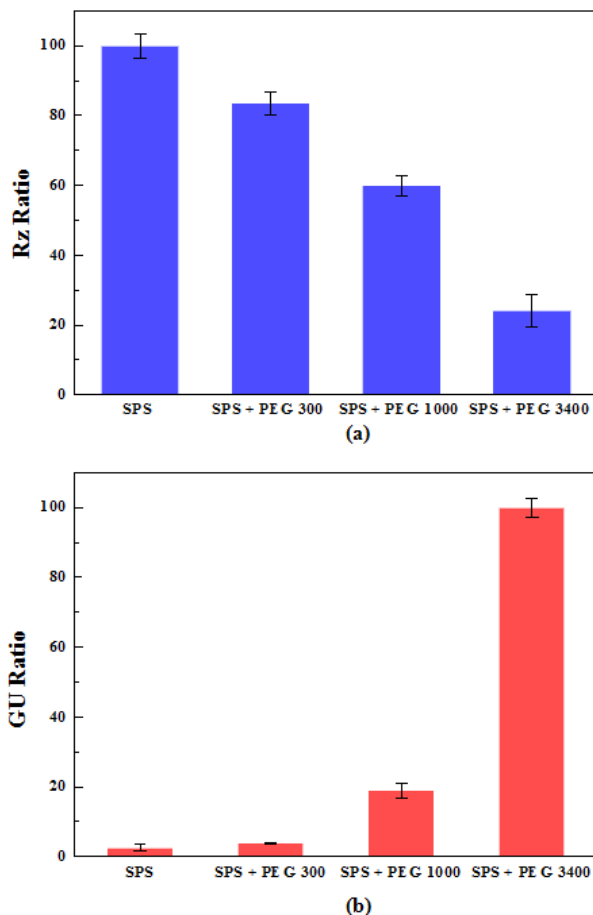### 3.3. The surface roughness and glossiness

Figure 3. Measured appearance features of electrodeposited copper foils with SPS and different PEG MW after 48 hours. (a) surface roughness and (b) glossiness.

Results of surface roughness and glossiness of electrodeposited copper foil are shown in Figure 3. The presence and MW of PEG were found to be related to both glossiness and surface roughness. The surface roughness was reduced when the MW of PEG MW was increased. Changes in surface roughness according to the MW of PEG were clearly observed in Figure 4.
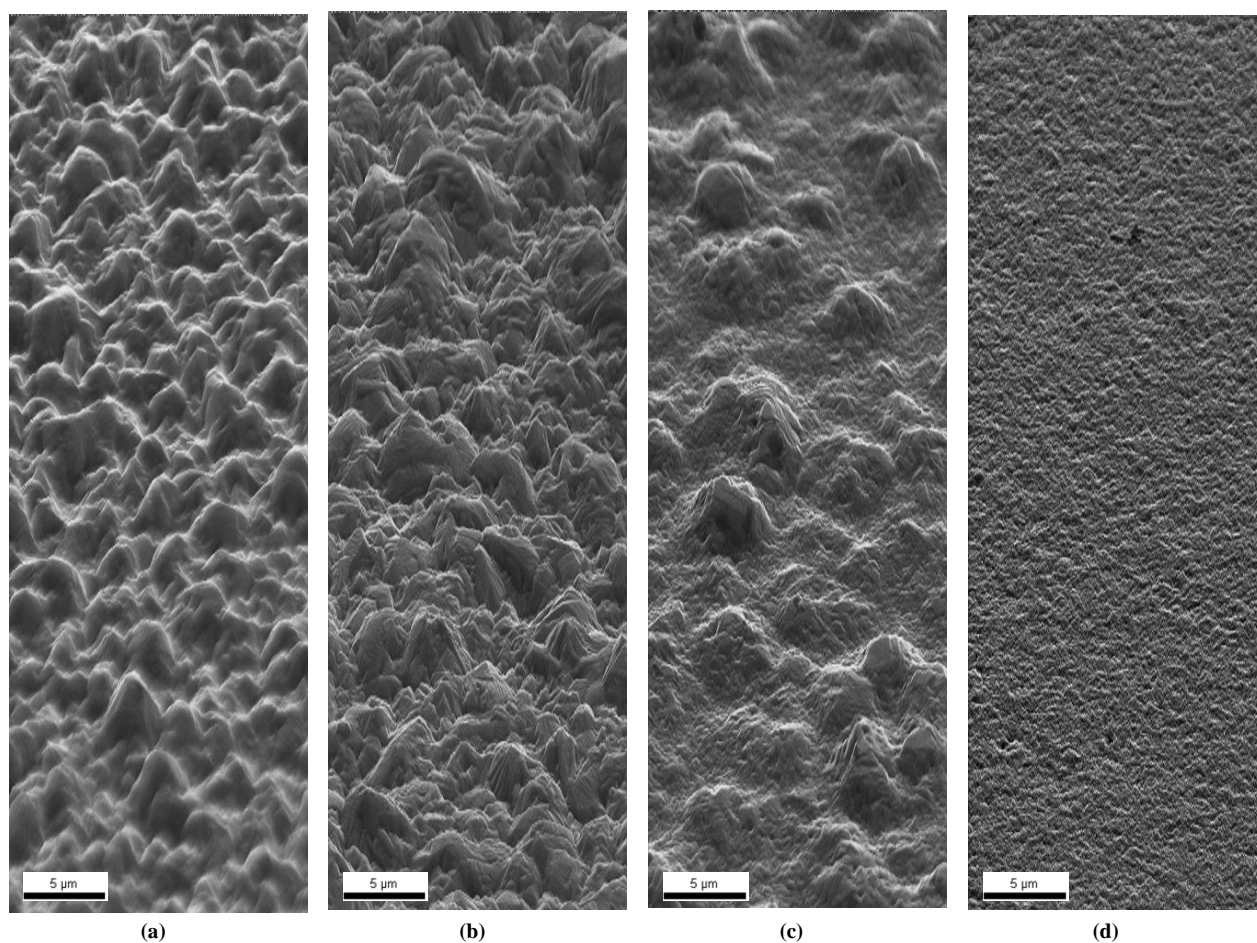

Figure 4. Degree of 70 tilted images of FE-SEM with various organic additives. (a) only SPS (b) SPS + PEG 300, (c) SPS + PEG 1000, and (d) SPS + PEG 3400
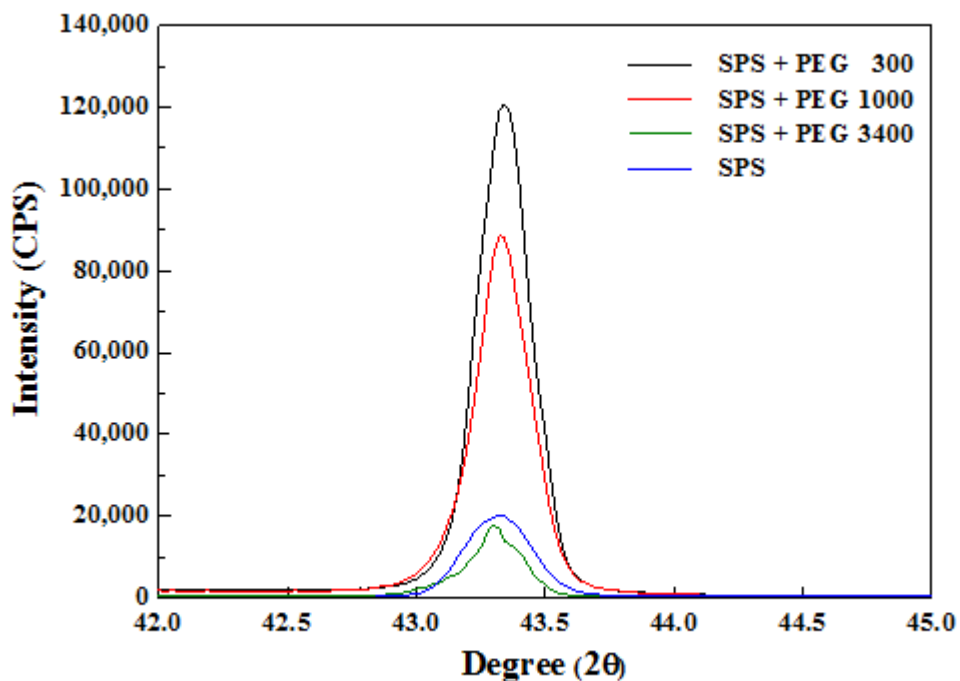
The glossiness is measured by the amount of light on the surface. Incident light from the glossmeter will be reflected to the surface. Only the regular reflection light is detected on a glossmeter [32]. As the surface roughness was reduced with increase in PEG MW, glossiness was increased.

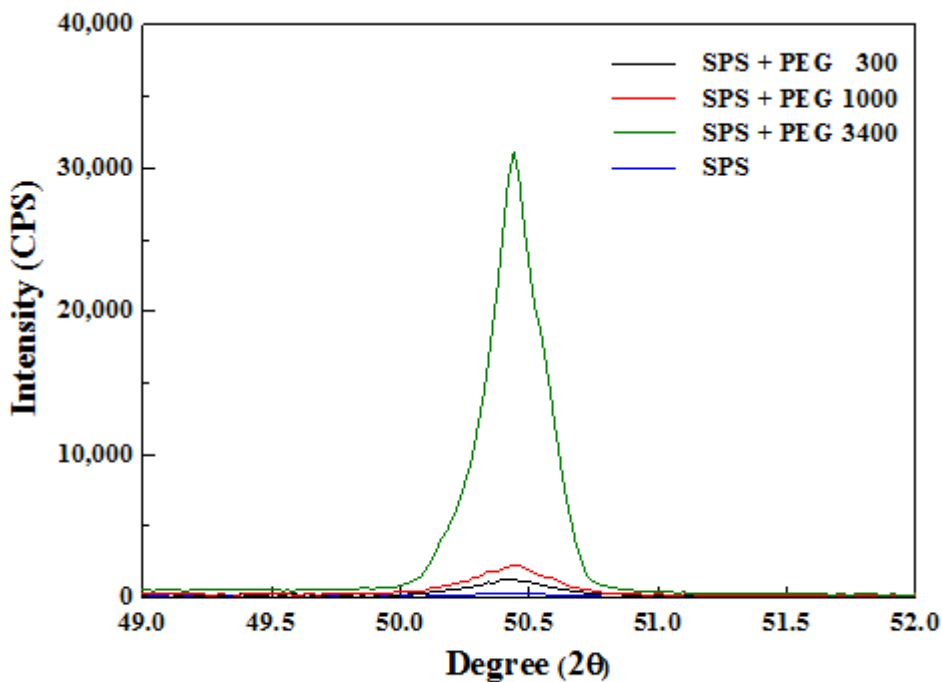### 3.4. Preferred crystallographic plane and grain size

In order to explain surface characteristics with organic additives, it is necessary to conduct microstructure analysis of the electrodeposited copper. XRD results of electrodeposited copper foils in plane 111 are shown in Figure 5a. In *Bravais* lattices, copper has a face-centered cubic (FCC) crystal

structure, of which plane 111 is a close-packed plane [33]. In consistent with this result, higher intensity of plane 111 compared to other planes was found in our study.

As mentioned in Quantum chemical analysis, the action of organic additives in SPS and PEG has an order. Preferentially, PEG acts on copper seed layer.
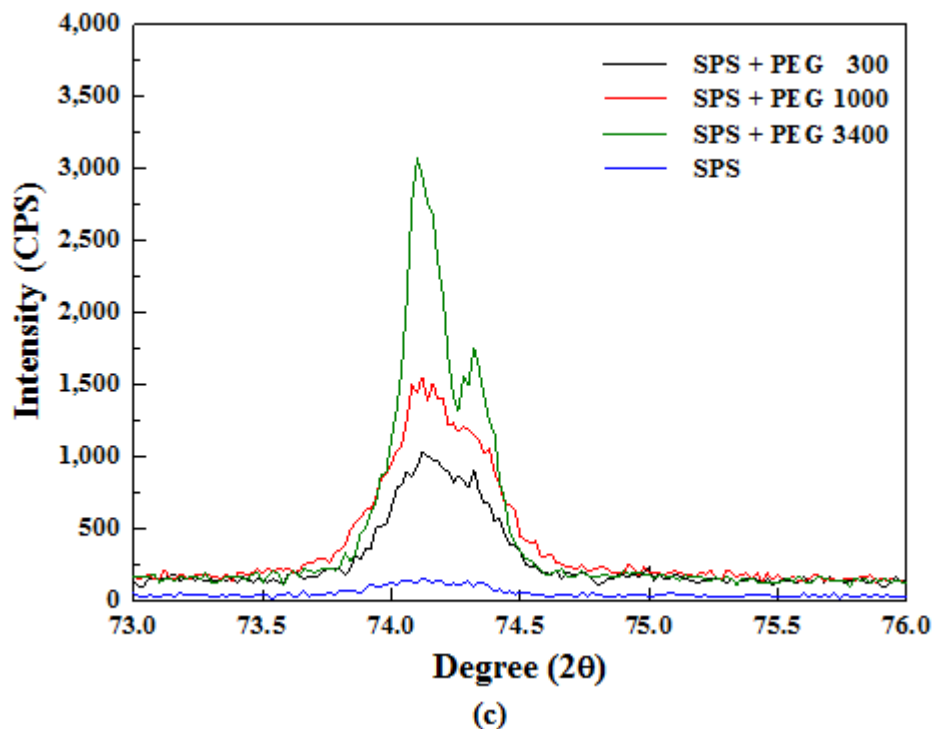

(a)

(b)

Figure 5. XRD pattern which represents the crystallographic orientation with SPS and different MW of PEG. Each plane is (a) (111), (b) (200), and (c) (220).

The inhibition reaction mechanisms of PEG have been reported in a number of studies [3,34,35]. The form of PEG - Cu^+ - Cl^- is structured as follows: two oxygen atoms of PEG are connected with cuprous ion, one chloride ion links between cuprous ion and copper surface. The functional group that traps the cuprous ions is an ether group that can inhibit copper electrodeposition. Larger MW of PEG means higher degree of polymerization and more ether groups, thus improving the inhibition effect. In addition, PEG adsorption onto copper substrate without cuprous ions is possible as long as chloride ions exist [36]. Depending on the mechanism, the reduction reaction of copper ions in the electrodeposition solution is dependent on the distribution of Cl^-. Because the atomic packing density is related to the adsorption reaction of Cl^-, the preferential absorption of Cl^- is on plane 111 [37,38]. Due to this adsorption of Cl^-, there is a possibility to make more PEG - Cu^+ - Cl^- complex on plane 111. Thus, the reduction reaction on plane 111 was more inhibited compared to that on plane 200 or plane 220. As the MW of PEG was increased, the growth inhibition on plane 111 might have worked more effectively that the intensity of XRD peak on plane 111 was decreased in Figure 5.

The PEG absorption reaction was followed by SPS acceleration reaction. This accelerating reaction improves the copper deposition rate on planes 111, 200, and 220. However, due to the PEG barrier, the SPS reaction on plane 111 was more delayed compared to that on plane 200 or plane 220. That is, the SPS reaction on planes 200 and 220 was more preferred than that on plane 111. Such plane preference was increased with higher MW of PEG due to difficulties in penetration. Among the three planes on FCC, the planar density was in an order of plane 111, 220 and 200. Consequently, higher MW of PEG changed the preferred crystallographic plane from 111 to 200. The relationship of electrodeposited copper surface feature with different MWs of PEG is shown in Figure 6b-d.
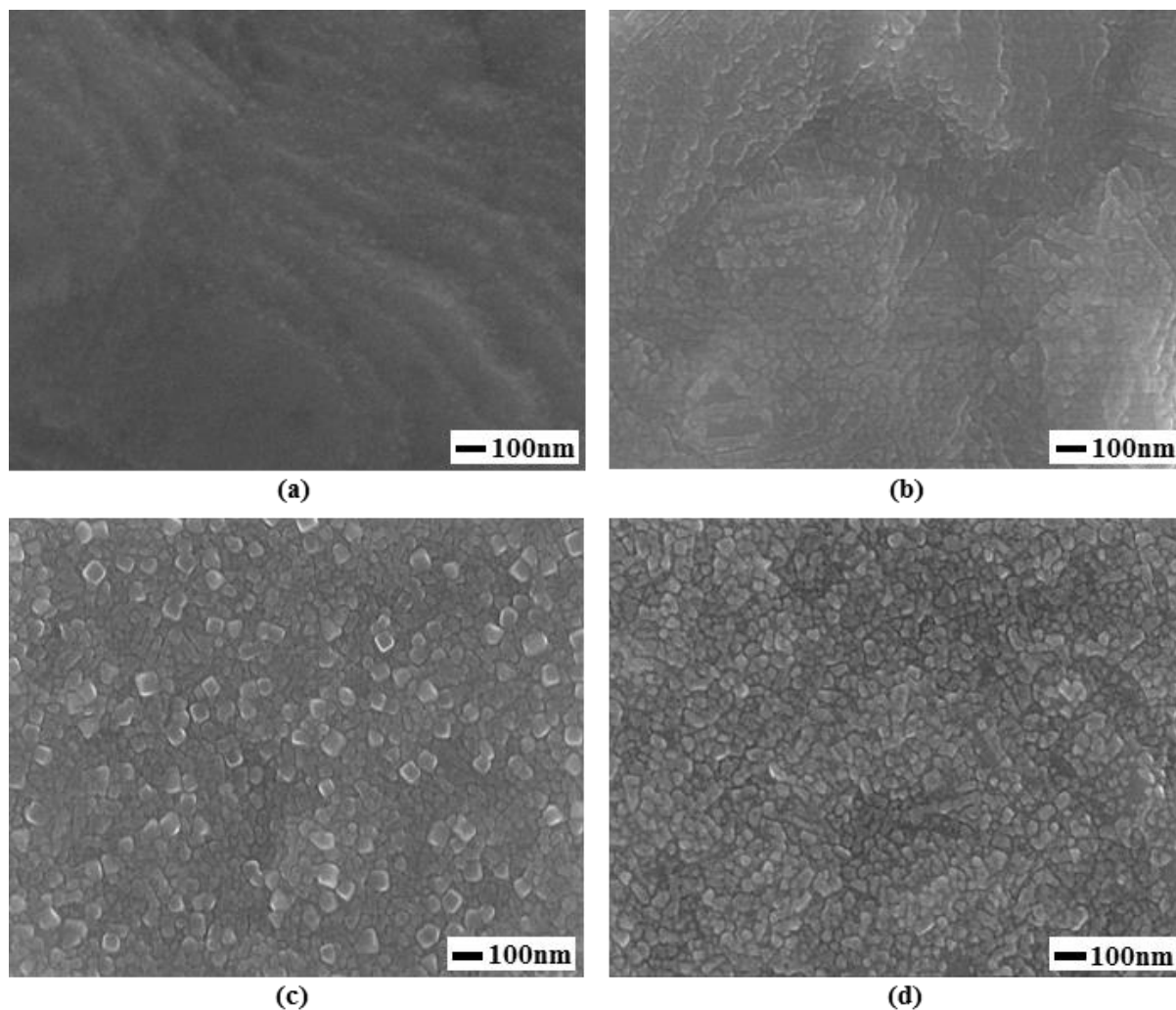
Figure 6. Top view images of FE-SEM with various organic additives. (a) only SPS (b) SPS + PEG 300, (c) SPS + PEG 1000, and (d) SPS + PEG 3400.

With higher MW, the cubic shape crystals were also increased. In FCC crystal structure, plane 111 had a triangular shape while planes 200 and 220 had rectangular shapes. In the XRD results, the increase of MW changed the preferred plane 200 that the cubic structure was expected at planes 200 and 220.

To estimate the grain size, the XRD results was interpreted with *Scherrer* equation:

$$\tau = \frac{0.9\lambda}{B\cos\theta}$$

(1)

where 0.9 is the shape factor, λ is the wavelength of Cu Kα, B is the full width at half maximum (FWHM), and θ is the angle. The relationship between the grain sizes in a percentage and MW of PEG in different planes is shown in Figure 7. The grain size on plane 111 showed similar values for all MWs of PEG. However, the grain size on planes 200 and 220 tended to be increased when the MW of PEG was increased. This is also due to the biasing action of SPS. The SPS energy needed to penetration PEG complex on plane 111 is larger than that on planes 200 or 220. Therefore, the acceleration reaction of SPS occurred more on planes 200 and 220 with more deposition of copper ions,

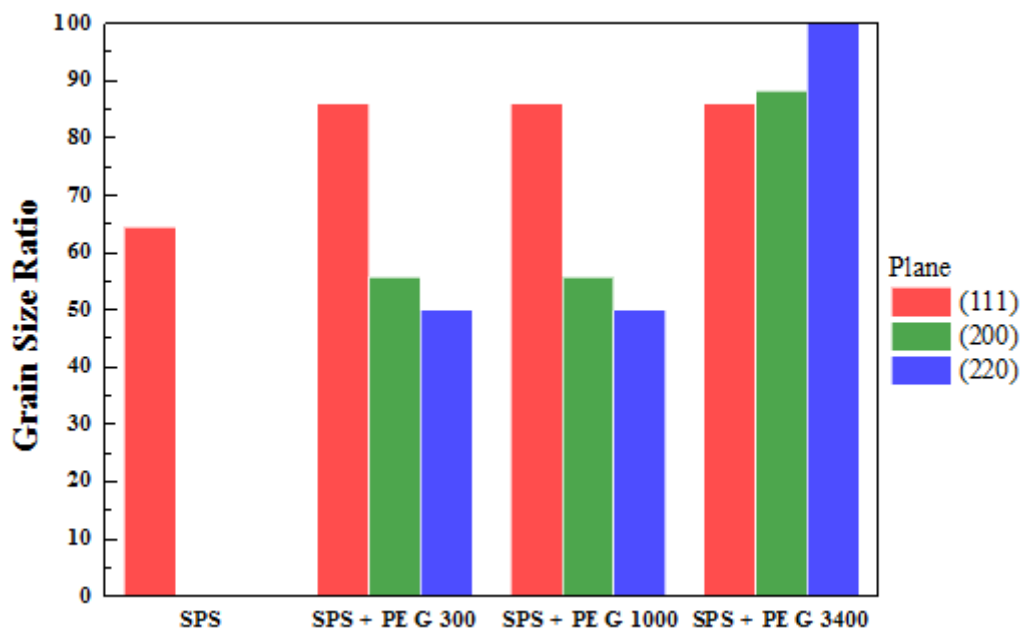thus more grains. When the MW of PEG was increased, more focused SPS reactions made more large grains.

Figure 7. Calculated grain size ratio of SPS and different MW of PEG in (111), (200) and (220) planes.

Based on the result of only SPS in Figure 5, the XRD intensity on plane 111 was similar to that of PEG-containing solutions or less. However, the XRD intensity on planes 200 and 220 was not revealed. Thus, in Figure 6a, crystallographic shape of rectangular was rarely observed. Figure 7 shows the grain size on plane 111 without PEG was smaller than that of PEG-containing specimens. These results mean that the absence of PEG can induce insufficient crystallographic growth and grain growth because the SPS-added solution is partially reacted during the copper electrodeposition. In this regard, the PEG worked as the suppressor while multiple amounts of SPS acted as the accelerator.

Previous study on correlation between grain size and roughness has revealed that more suppression effect of PEG will reduce the surface roughness due to smaller grain size [39,40]. However, our XRD results revealed that the surface roughness was more influenced by the preferred plane than by the reduced grain size when accelerator and suppressor co-existed.

4. CONCLUSION

The influence of different MW PEG on the copper electrodeposition with SPS and Cl⁻ was investigated using quantum analysis, cyclic voltammetry, XRD, and SEM. It comes down to the following conclusions:

1.   Quantum analysis and cyclic voltammetry revealed that higher MW of PEG increased

the effect of inhibition regardless of the existence of SPS, indicating that the adsorption property of PEG is not related to other additives but to the increases of ether group in the form of PEG - Cu^+ - Cl^-.

2.   The increase of suppression capacity affected surface nature. When the MW of PEG was increased, the surface roughness is decreased while the glossiness was increased. Based on XRD analysis, the cause of this phenomenon was greatly influenced by the preferred plane rather than grain size.

3.   The difference in the PEG adsorption nature according to its MW affected the concentration of SPS. As the degree of adsorption was increased, the biasing of SPS on planes 200 or 220 was accelerated because more PEG was adsorbed on plane 111 due to chloride ions. The number of cubic shape grain at planes 200 and 220 was increased as the PEG MW was increased.

4.   SPS without PEG resulted in insufficient crystallographic growth and grain growth. Therefore, PEG activated the SPS reaction by increasing the amount of working SPS.

References

1.   Y. D. Gamburg and G. Zangari, *Theory and Practice of Metal Electrodeposition*, Springer, New York (2011).
2.   R. S. Khandpur, *Printed Circuit Boards: Design, Fabrication, Assembly and Testing*, McGraw-Hill, New Delhi (2005).
3.   M. A. Pasquale, L. M. Gassa and A. J. Arvia, *Electrochim. Acta,* 53 (2008) 5891.
4.   N. T. M. Hai, J. Odermatt, V. Grimaudo, K. W. Krämer, A. Fluegel, M. Arnold, D. Mayer and P. Broekmann, *J. Phys. Chem. C*, 116 (2012) 6913.
5.   M. Schlesinger and M. Paunovic, *Modern electroplating*, Wiley, New Jersey (2010).
6.   T. Liang, S. Hall, H. Heck and G. Brist, A practical method for modeling PCB transmission lines with conductor surface roughness and wideband dielectric properties, 2006 IEEE MTT-S International Microwave Symposium Digest, San Francisco, USA, 2006, 1780
7.   S. Hinaga, M. Y. Koledintseva, P. K. R. Anmula and J. L. Drewniak, Effect of conductor surface roughness upon measured loss and extracted values of PCB laminate material dissipation factor, Proceedings of the Technical Conference, Las Vegas, USA, 2009
8.   S. J. Normyle, T. F. McCarthy and D. L. Wynants, The impact of conductor surface profile (Rrms) on total circuit attenuation in microstrip and stripline transmission lines, Taconic Advanced Dielectric Division, New York, USA, 2006
9.   H. Johnson and M. Graham, *High-speed signal propagation: advanced black magic*, Prentice Hall, New Jersey (2003).
10. M. Paunovic and M. Schlesinger, *Fundamentals of electrochemical deposition*, Wiley, New Jersey (2006).
11. D. M. Soares, S. Wasle, K. G. Weil and K. Doblhofer, *J. Electroanal. Chem.,* 532 (2002) 353.
12. W. Shao, G. Pattanaik and G. Zangari, *J. Electrochem. Soc.*, 154 (2007) D201.
13. W. P. Dow and H. S. Huang, *J. Electrochem. Soc.*, 152 (2005) C67.
14. W. Chu, M. S. Moats, A. Luyima and C. Heckman, *Miner. Metall. Process*, 33 (2016) 31.
15. M. Tan, C. Guymon, D. R. Wheeler and J. N. Harb, *J. Electrochem. Soc.*, 154 (2007) D78.
16. S. L. Ko, J. Y. Lin, Y. Y. Wang and C. C. Wan, *Thin Solid Films*, 516 (2008) 5046.
17. R. Manu and S. Jayakrishnan, *Bull. Mater. Sci.*, 34 (2011) 347.
18. C. F. Hsu, W. P. Dow, H. C. Chang and W. Y. Chiu, *J. Electrochem. Soc.*, 162 (2015) D525.
19. M. K. Awad, *Can. J. Chem.*, 91 (2013) 283.
20. S. Lagrange, S. H. Brongersma, M. Judelewicz, A. Saerens, I. Vervoort, E. Richard, R. Palmans an

d K. Maex, *Microelectron. Eng.*, 50 (2000) 449.
21. M. Stangl, J. Acker, V. Dittel, W. Gruner, V. Hoffmann and K. Wetzig, *Microelectron. Eng.*, 82 (2005) 189.
22. V. A. Vas'ko, I. Tabakovic, S. C. Riemer and M. T. Kief, *Microelectron. Eng.*, 75 (2004) 71.
23. A. K. Sikder, A. Kumar, P. Shukla, P. B. Zantye and M. Sanganaria, *J. Electron. Mater.*, 32 (2003) 1028.
24. J. Zeng, R. Q. Zhang and H. R. Treutlein, *Quantum simulations of materials and biological systems*, Springer, New York (2012).
25. N. Kovacevic and A. Kokalj, *Corros. Sci.*, 53 (2011) 909.
26. C. Wang, J. Zhang, P. Yang and M. An, *Electrochim. Acta*, 92 (2013) 356.
27. M. Finsgar, A. Lesar, A. Kokalj and I. Milosev, *Electrochim. Acta*, 53 (2008) 8287.
28. Y. D. Chiu and W. P. Dow, *J. Electrochem. Soc.*, 160 (2012) D3021.
29. Y. F. Liu, K. Krug, P. C. Lin, Y. D. Chiu, Y. L. Lee and W. P. Dow, *J. Phys. Chem. C*, 115 (2011) 7638.
30. P. Broekmann, A. Fluegel, C. Emnet, M. Arnold, C. R. Goepfert, A. Wagner, N. T. M. Hai and D. Mayer, *Electrochim. Acta*, 56 (2011) 4724.
31. Chrzanowska and R. Mroczka, *Electrochim. Acta*, 78 (2012) 316.
32. A. A. Maradudin, *Light Scattering and Nanoscale Surface Roughness*, Springer, New York (2007).
33. W. D. Callister and D. G. Rethwisch, *Fundamentals of Materials Science and Engineering*, Wiley, New Jersey (2008).
34. Z. V. Feng, X. Li and A. A. Gewirth, *J. Phys. Chem. B*, 107 (2003) 9415.
35. K. R. Hebert, S. Adhikari and J. E. Houser, *J. Electrochem. Soc.*, 152 (2005) C324.
36. K. Kondo, R. N. Akolkar, D. P. Barkey and M. Yokoi, *Copper Electrodeposition for Nanofabrication of Electronic Devices*, Springer, New York (2014).
37. J. M. Song, Y. S. Zou, C. C. Kuo and S. C. Lin, *Corros. Sci.*, 74 (2013) 223.
38. S. M. Mayanna and T. H. V. Setty, *Corros. Sci.*, 14 (1974) 691.
39. M. S. Kang, S. K. Kim, K. H. Kim and J. J. Kim, *Thin Solid Films*, 516 (2008) 3761.
40. K. W. Chen, Y. L. Wang, L. Chang, F. Y. Li and S. C. Chang, *Surf. Coat. Technol.*, 200 (2006) 3112.